Tau neutrino

Adriano Cherchiglia,[1] O. L. G. Peres,[1] and E. S. Souza[1]
[1]*Instituto de Física Gleb Wataghin - UNICAMP, 13083-859, Campinas SP, Brazil*

I. MOTIVATION

In the paper from Andre de Gouvea *et al.* (1904.07265)[1], they compute the number of tau neutrinos in the far detector (fig.2 in the paper). Here the Figure(1). The figure has two curves, one for the true energy of the incident neutrino (dashed) and the other for the reconstructed energy(solid). The decay chain is something like:

$$\nu_\tau N \to \tau + X \tag{1}$$

where $\tau \to \nu_\tau +$ hadron. We do not measure the tau, only the hadronic debris. Therefore, we cannot reconstruct the energy of the incident neutrino very well (part of the energy is lost in the final neutrino). This explains why the solid curves are to the the left of the dashed ones. For the plots, we have

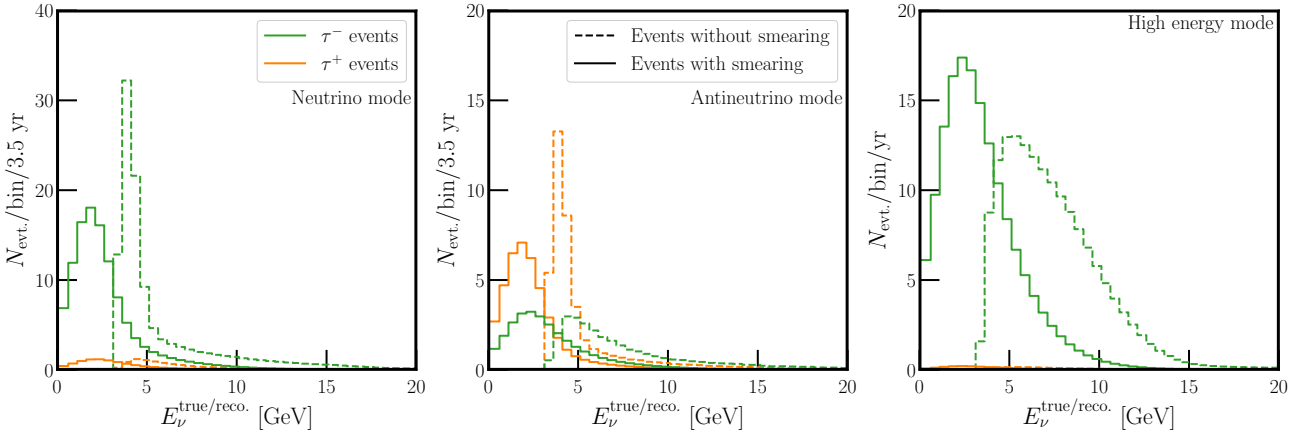

FIG. 1. Expected number of ν_τ-identified signal events per 0.5 GeV bin as a function of the true (dashed) or reconstructed (solid) neutrino energy. The left panel displays the expected number of events when in neutrino mode, the center panel displays the antineutrino mode, and the right panel displays high-energy mode events. In each panel, we show the contribution due to neutrinos in green and antineutrinos in orange. Each distribution has been normalized to the expected run-time in each mode, 3.5 years for neutrino and antineutrino modes and 1 year for high-energy mode.

$$N_{\text{events}}^{\text{SM}} = \phi_\mu P(\nu_\mu \to \nu_\tau)\sigma_\tau \tag{2}$$

since in the SM, there is no tau neutrino at source. So, the tau neutrino only appears at the far detector through conversion. In our model, we have

$$P_{\mu\beta}^{\text{NSI}} = \left| S_{\beta\mu}^{\text{SM}} - p_\mu \epsilon_{\mu i}^* S_{\beta i}^{\text{SM}} \right|^2, \tag{3}$$

where we have a sum over i.

II. THE MODEL

The EFT Lagrangian that modifies the neutrino interactions is defined by [2]

$$\begin{aligned}\mathscr{L}_{\text{WEFT}} \supset -\frac{2\,V_{jk}^{CKM}}{v^2}\Big\{&[1+\epsilon_L^{jk}]_{\alpha\beta}\left(\bar{u}^j\gamma^\mu P_L d^k\right)\left(\bar{\ell}_\alpha\gamma_\mu P_L\nu_\beta\right) + [\epsilon_R^{jk}]_{\alpha\beta}\left(\bar{u}^j\gamma^\mu P_R d^k\right)\left(\bar{\ell}_\alpha\gamma_\mu P_L\nu_\beta\right)\\ &+\frac{1}{2}\left[\epsilon_S^{jk}\right]_{\alpha\beta}\left(\bar{u}^j d^k\right)\left(\bar{\ell}_\alpha P_L\nu_\beta\right) - \frac{1}{2}\left[\epsilon_P^{jk}\right]_{\alpha\beta}\left(\bar{u}^j\gamma^5 d^k\right)\left(\bar{\ell}_\alpha P_L\nu_\beta\right)\\ &+\frac{1}{4}\left[\epsilon_T^{jk}\right]_{\alpha\beta}\left(\bar{u}^j\sigma^{\mu\nu} P_L d^k\right)\left(\bar{\ell}_\alpha\sigma_{\mu\nu} P_L\nu_\beta\right) + \text{h.c.}\Big\}\,.\end{aligned} \tag{4}$$

Here, V^{CKM} is the Cabibbo-Kobayashi-Maskawa (CKM) matrix, $v = 1/(\sqrt{2}G_F) \approx 246\,\text{GeV}$ is the vacuum expectation value of the SM Higgs field and ϵ_X are the Wilson coeficients, with $X = L, R, S, P, T$ for left-handed, right-handed, scalar, pseudo-scalar and tensor, respectively. The Roman (Greek) symbols denote the quark (lepton) generations. This Lagrangian is based on the Weak Effective Field Theory (WEFT), that acts bellow electroweak scale [3].

For simplicity, we only study $(\epsilon_P)_{\alpha\beta}$ which we will denote as $\epsilon_{\alpha\beta}$.

III. METHODOLOGY

We have extracted from the plots of fig. I the number of true events as well as the reconstructed ones for all channels. The latter is only needed for cross-check. Using the number of true events as input, we have obtained the reconstructed events by ourselves. This was achieving by a smearing function given by

$$f(E_{\rm rec}, E_{\rm true}) = \exp\left[-\frac{1}{2}\left(\frac{E_{\rm rec} - bE_{\rm true})}{rE_{\rm true}}\right)^2\right] \tag{5}$$

where $b = 0.45$, and $r = 0.25$.

Explicitly,

$$\frac{dN_{\rm events}}{dE_\nu^{\rm reco}} = \int {\rm d}E_\nu^{\rm true} \frac{dN_{\rm events}}{dE_\nu^{\rm true}} f(E_{\rm rec}, E_{\rm true}) \tag{6}$$

We have checked that the points reconstructed by ourselves in this way agree with the reconstructed points of the plots of fig I. Normalization factors were added, to guarantee that the total number of reconstructed events is the same as the true events.

In the plots, the following parameters were fixed

$$\begin{gathered} \sin^2\theta_{12} = 0.310; \quad \sin^2\theta_{13} = 0.02240; \quad \sin^2\theta_{23} = 0.582; \\ \delta_{\rm CP} = -2.50{\rm rad} \quad \Delta m^2_{21} = 7.39\times10^{-5}{\rm eV}^2 \quad \Delta m^2_{31} = 2.525\times10^{-3}{\rm eV}^2 \end{gathered} \tag{7}$$

The baseline is 1300km for DUNE as well as the matter density is $\rho = 2.848 g/cm^3$.

It is possible to obtain the number of events for other values by re-scaling as below

$$\frac{dN_{\rm events}(\hat{x})}{dE_\nu^{\rm true}} = \phi_\mu P^{\hat{x}}_{\mu\tau}\sigma_\tau = \frac{P^{\hat{x}}_{\mu\tau}}{P^{x}_{\mu\tau}} \frac{dN_{\rm events}(x)}{dE_\nu^{\rm true}} \tag{8}$$

where x is a vector with the parameters defined in Eq. (7), while $\hat{x}$ is a vector with a different choice for any of the parameters. In the presence of NSI, it is still possible to obtain a perturbative formula for the conversion probability. Or one can resort to numerical methods. In any case, it is straightforward to obtain the event rates for any chosen value of the standard parameters or/and NSI.

Once the number of events from CC is known, we have to add the background (NC). It can be extracted from the figure (black region)

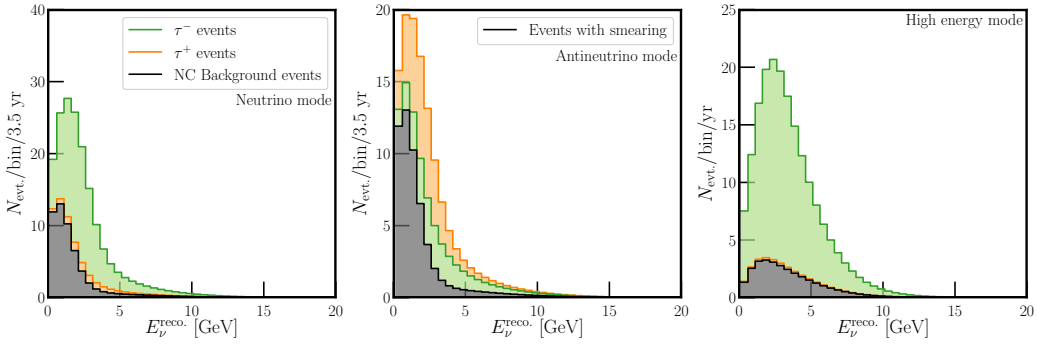

FIG. 2. Caption

Finally, the chi square function is given by

$$\chi^2 = \sum_i n_{i,teo} - n_{i,data} + n_{i,data}\log\left(\frac{n_{i,data}}{n_{i,teo}}\right) + \left(\frac{\alpha}{\sigma}\right)^2 \tag{9}$$

where $n_{i,teo} = N_i^{NSI} = N_{i,CC}^{NSI} + (1+\alpha)N_{i,NC}^{NSI}$, and $n_{i,data} = N_i^{SM} = N_{i,CC}^{SM} + N_{i,NC}^{SM}$. We also chose $\sigma = 0.25$

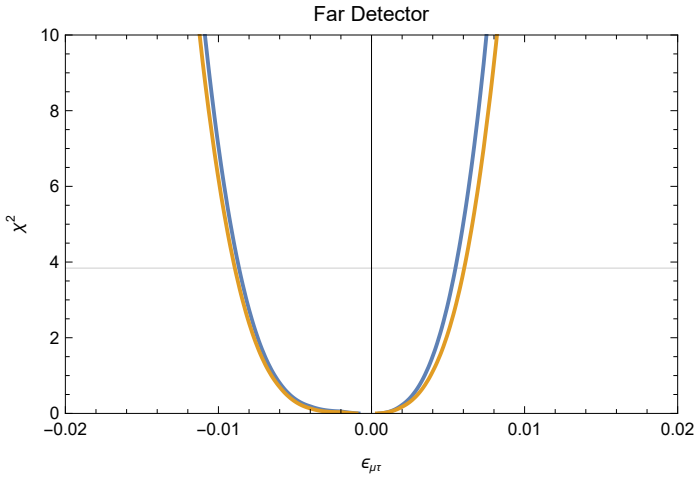

FIG. 3. Sensitivity on $\epsilon_{\mu\tau}$ at the far detector, considering running of 3. years at neutrino mode, 3. years at anti-neutrino mode, and 1 year at high-energy mode. The line is for 95%C.L. The blue line is without background and the orange line is including background.

The above analysis was applied to study the sensitivity on $\epsilon_{\mu\tau}$. Fixing the values of the standard parameters as in Eq. (7) we obtained the result of fig. 3.(preliminary result)

The current bound (from pion decay) is around 2×10^{-3} at 90%C.L. [3]. The sensitivity from DUNE is at least one order of magnitude higher.

We can also study the sensitivity at the near detector. In this case, we can obtain the number of events by the formula

$$\frac{dN^{near}_{\text{events}}(\hat{x})}{dE^{\text{true}}_{\nu}} = \phi^{near}_{\mu} P^{\hat{x}}_{\mu\tau}\sigma_{\tau} = \frac{P^{\hat{x}}_{\mu\tau}}{P^{x}_{\mu\tau}}\frac{\phi^{near}_{\mu}}{\phi^{far}_{\mu}}\frac{dN_{\text{events}}(x)}{dE^{\text{true}}_{\nu}} \tag{10}$$

We will approximate the flux as spherically symmetry, so $N = \int \phi^{total} dA \rightarrow \phi^{total} = N/(4\pi r^2)$. Moreover, the detector can only see a fraction of the flux. Thus,

$$\frac{\phi^{near}_{\mu}}{\phi^{far}_{\mu}} = \frac{N_{near}/(4\pi r^2_{near})}{N_{far}/(4\pi r^2_{far})} = \frac{N_{near}}{N_{far}}\frac{r^2_{far}}{r^2_{near}} \equiv \kappa \tag{11}$$

We will consider that $L_{near} = 1$km, and that the near detector will contain 70 ton while $N_{\text{far}} = 40$ kton. This is particularly interesting, since the standard event rate is very small. We obtain the result of fig. 4preliminary result

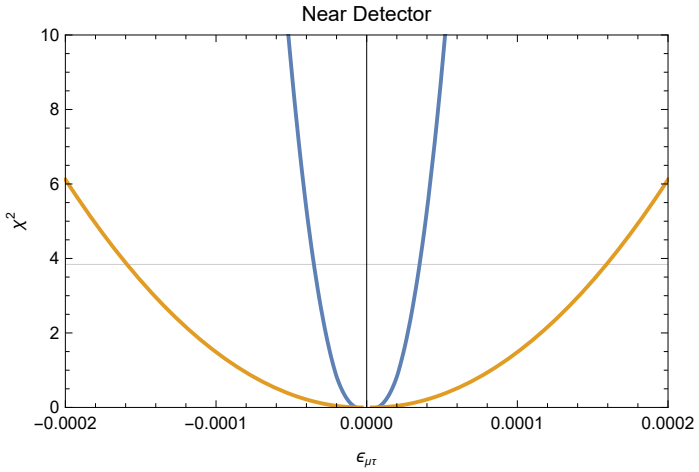

FIG. 4. Sensitivity on $\epsilon_{\mu\tau}$ at the near detector, considering running of 3. years at neutrino mode, 3. years at anti-neutrino mode, and 1 year at high-energy mode. The line is for 95%C.L. The blue line is without background and the orange line is including background.

From the result above, DUNE could increase the sensitivity on $\epsilon_{\mu\tau}$ one order of magnitude. preliminary

When computing the result for the far detector, we are implicitly using the normalization for fluxes (of muon neutrino) in the SM. Since the fluxes change, we have to take this into account as well.

Recall that we defined

$$\frac{dN^{\rm near}_{\rm events}(\hat{x})}{dE^{\rm true}_{\nu}} = \phi^{near}_{\mu}(x) P^{\hat{x}}_{\mu\tau}\sigma_{\tau} \tag{12}$$

however, we should have used

$$\frac{dN^{near}_{\rm events}(\hat{x})}{dE^{\rm true}_{\nu}} = \phi^{near}_{\mu}(\hat{x}) P^{\hat{x}}_{\mu\tau}\sigma_{\tau} = \frac{P^{\hat{x}}_{\mu\mu}}{P^{x}_{\mu\mu}}\phi^{near}_{\mu}(x) P^{\hat{x}}_{\mu\tau}\sigma_{\tau} \tag{13}$$

$$\frac{dN^{far}_{\rm events}(\hat{x})}{dE^{\rm true}_{\nu}} = \phi^{far}_{\mu}(\hat{x}) P^{\hat{x}}_{\mu\tau}\sigma_{\tau} \;=\; \frac{\phi^{far}_{\mu}(\hat{x})}{\phi^{near}_{\mu}(\hat{x})}\frac{\phi^{near}_{\mu}(\hat{x})}{\phi^{near}_{\mu}(x)}\frac{\phi^{near}_{\mu}(x)}{\phi^{far}_{\mu}(x)}\phi^{far}_{\mu}(x) P^{\hat{x}}_{\mu\tau}\sigma_{\tau} \tag{14}$$

$$\;=\; \kappa^{-1}\,\frac{P^{\hat{x}}_{\mu\mu}}{P^{x}_{\mu\mu}}\,\kappa\,\phi^{far}_{\mu}(x) P^{\hat{x}}_{\mu\tau}\sigma_{\tau} = \frac{P^{\hat{x}}_{\mu\mu}}{P^{x}_{\mu\mu}}\,\phi^{far}_{\mu}(x) P^{\hat{x}}_{\mu\tau}\sigma_{\tau} \tag{15}$$

We have also checked what is the ratio ϕ^{near}/ϕ^{far} using the implementation in GLOBES of DUNE [**?**], see fig 5. In the figure, the red line is for $(1300/1)^2$, while the green line is for $(1297/0.574)$ which are the values used in GLOBES implementation (see section II of [**?**]). The energy displayed in the plots is the true energy. Moreover, our choice to use only geometric factors is conservative for most of the points (the points are above the green line).

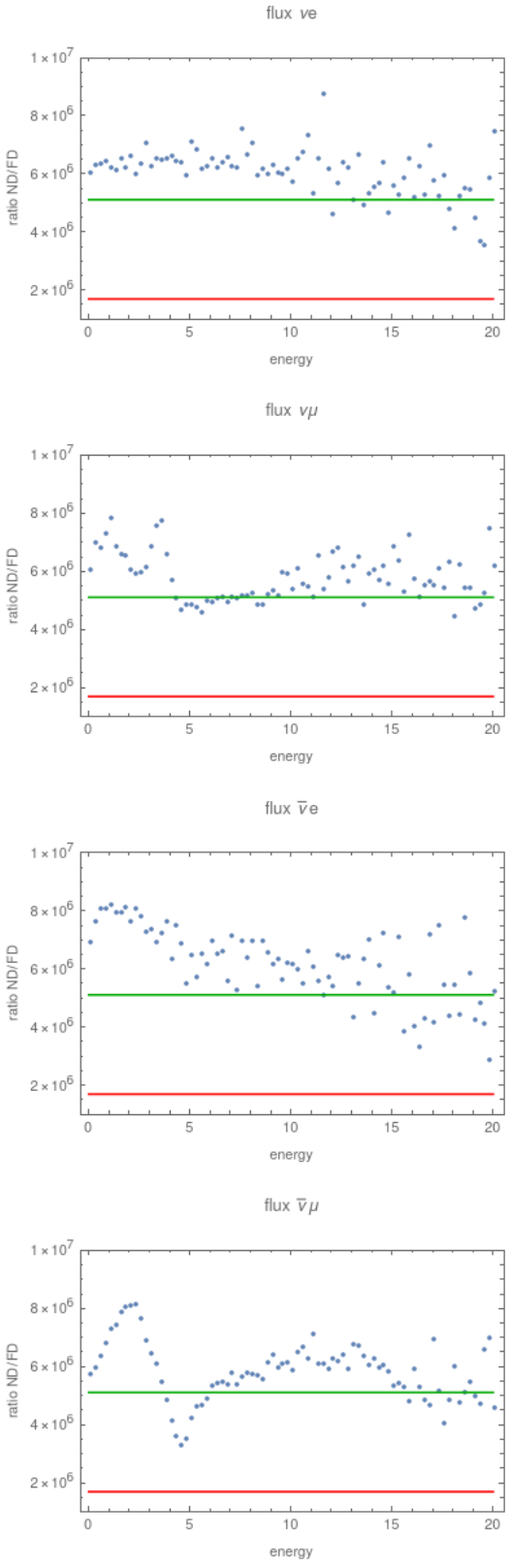

FIG. 5. Ratio flux near/far from DUNE

Using GLOBES, we can also study which is the sensitivity on $\epsilon_{\mu\tau}$. The results are given in figures 6-7. In fig. 6, the standard parameters are fixed in the best-fit check values, while in fig. 7 the std parameters are allowed to vary at 1sg, need checking. In GLOBES, they consider 10 years, not 7 as we are doing. There is not high energy as well.

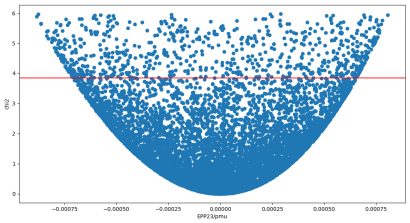

FIG. 6. Fixed std

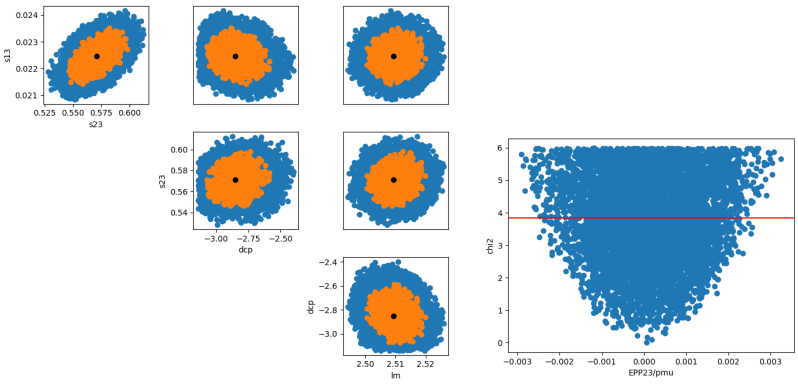

FIG. 7. Free std

Next job is to study the disapparence rate, how it change with NSI.

IV. NEUTRINO TRANSITION RATE

Copied from 2309.15924

In this work we will adopt the more general QFT framework to describe neutrino oscillations in long-baseline experiments, following [2] (see also [4–6] for previous treatment in QFT not including NSI). The main point is to consider the entire process (from neutrino production to its detection) as an unique process in QFT. Thus, the differential event rate for neutrinos of flavor β with energy E_ν to be detected at a distance L from the source S, where they were produced with flavor α, is given by

$$R^S_{\alpha\beta} = \frac{N_T}{32\pi L^2 m_S m_T E_\nu} \sum_{k,l} e^{-i\frac{L\Delta m^2_{kl}}{2E_\nu}} \int d\Pi_{P'} \mathscr{M}^P_{\alpha k} \overline{\mathscr{M}}^P_{\alpha l} \int d\Pi_D \mathscr{M}^D_{\beta k} \overline{\mathscr{M}}^D_{\beta l} \,, \tag{16}$$

where N_T is the number of target particles, $m_{S,T}$ are the masses of the source and target particles respectively, and we denote complex conjugation with a bar. As usual, $\Delta m^2_{kl} \equiv m^2_k - m^2_l$ denotes the difference of neutrino masses squared, while the phase-space integrals are given by $d\Pi \equiv \frac{d^3k_1}{(2\pi)^3 2E_1} \cdots \frac{d^3k_n}{(2\pi)^3 2E_n} (2\pi)^4 \delta^4(\sum p_n - \sum k_i)$. Here, we denote by k_i and E_i the four-momenta and energies of the final states, while the sum $\sum p_n$ amounts to the total four-momentum of the initial state. Since we are interested in the differential number of events per incident neutrino energy E_ν, we actually define $d\Pi_P \equiv d\Pi_{P'} dE_\nu$, as can be seen in eq.(16). Notice also that we are considering oscillation in vacuum only. Matter effects will be taken into account below.

As already stated, we will focus on long-baseline experiments, in which neutrinos are mainly produced by pion decay. Moreover, we will only consider beyond the SM (BSM) possible effects at neutrino production and/or propagation (by interaction with the medium). This is justified by the complicated nature of detection in long-baseline experiments. To properly include BSM effects, it would require first a theoretical description of standard neutrino interaction with nucleus, which is still not

satisfactory [7](see appendix **??** a brief description of the present status). Thus, regarding the detection amplitude, $\mathscr{M}^D_{\beta k}$, it will be given by

$$\mathscr{M}^D_{\beta k} = U_{\beta k} A^D \,, \tag{17}$$

where A^D is a reduced matrix element whose explicit form is not relevant, and U_{ij} is the PMNS matrix.

As recently pointed out [8], in the presence of BSM effects care must be exercised when calculating the phase-space integral related to the production amplitude. The amplitude concerning pion decay, $\pi^+ \to \ell^+_\alpha \nu_k$, is given by [8]

$$\mathscr{M}^{P,\pi}_{\alpha k} \equiv \mathscr{M}(\pi^+ \to \ell^+_\alpha \nu_k) = -i\, m_\mu f_{\pi^\pm} \frac{V_{ud}}{v^2} [\mathscr{P} U]^*_{\alpha k} (\bar{u}_{\nu_k} P_L v_{\ell_\alpha}) \,, \tag{18}$$

where $f_{\pi^\pm}$ is the pion decay constant, v_{ℓ_α}, $\bar{u}_{\nu_k}$ are the Dirac spinor wave functions of the charged lepton and the neutrino, respectively, and we are using the notation

$$[\mathscr{P}]_{\alpha\beta} \;\equiv\; \delta_{\alpha\sigma} + \bar{\epsilon}_{\alpha\sigma}, \quad \text{where} \quad \bar{\epsilon}_{\alpha\sigma} = (\epsilon_L)_{\alpha\sigma} - (\epsilon_R)_{\alpha\sigma} - \frac{m^2_{\pi^\pm}}{m_{\ell_\alpha}(m_u + m_d)} (\epsilon_P)_{\alpha\sigma} \,. \tag{19}$$

The NSI $\epsilon_L, \epsilon_R, \epsilon_P$ are defined in eq.(**??**). As can be seen, $\bar{\epsilon}_{\alpha\sigma}$ actually encodes the deviation from the PMNS matrix U due to the presence of NSI.

At first sight, one could insert eq.(18) into eq.(16), perform the phase-space integration, and obtain that BSM effects appear only in the numerator of eq.(16). However, this reasoning is incorrect, since we are assuming the BSM presence in all cases that the pion decay is involved, related (or not) to experiments that aim to probe neutrinos properties. Therefore, we should re-express eq.(18) in terms of the experimental measured decay width of the pion, which was already affected by BSM effects as well. Proceeding this way, we obtain [8]

$$\int d\Pi_{P'} \mathscr{M}^{P,\pi}_{\alpha k} \bar{\mathscr{M}}^{P,\pi}_{\alpha l} = 2\, m_{\pi^\pm} \Gamma_{\pi \to \ell_\alpha \nu} \frac{[\mathscr{P} U]_{\alpha l} [U^\dagger \mathscr{P}^\dagger]_{k\alpha}}{[\mathscr{P}\mathscr{P}^\dagger]_{\alpha\alpha}} \, \delta\Big(E_\nu - E_{\nu,\pi}\Big) \,, \tag{20}$$

where $E_{\nu,\pi} = (m^2_{\pi^\pm} - m^2_\alpha)/(2 m_{\pi^\pm})$ stands for the energy of the neutrino emitted. Finally, we can write eq.(16) in the form

$$R^S_{\alpha\beta} = N_T \sigma^{\rm SM}_\beta(E_\nu) \Phi^{\rm SM}_\alpha(E_\nu) \sum_{k,l} e^{-i \frac{L \Delta m^2_{kl}}{2E_\nu}} \frac{[\mathscr{P} U]_{\alpha l} [U^\dagger \mathscr{P}^\dagger]_{k\alpha}}{[\mathscr{P}\mathscr{P}^\dagger]_{\alpha\alpha}} U_{\beta k} U^*_{\beta l} \,, \tag{21}$$

where $\Phi^{\rm SM}_\alpha$ is the SM flux (with the decay width of the pion, $\Gamma_{\pi \to \ell_\alpha \nu}$, as input), while $\sigma^{\rm SM}_\beta$ is the SM cross-section. Notice that, by including the indirect effects (the denominator in $R^S_{\alpha\beta}$), there is no sensitivity to diagonal-only NSI.

V. TO DO

- We can re-scale the plots simply by doing

$$N^{\rm NSI}_{\rm events} = \phi_\mu P^{\rm NSI}_{\mu\tau} \sigma_\tau = \frac{P^{\rm NSI}_{\mu\tau}}{P^{\rm SM}_{\mu\tau}} N^{\rm SM}_{\rm events} \tag{22}$$

  So the first step is to compute the ratio $\frac{P^{\rm NSI}_{\mu\tau}}{P^{\rm SM}_{\mu\tau}}$ using the oscillation parameters in the paper as a function of the energy. They used

$$\begin{gathered} \sin^2\theta_{12} = 0.310; \quad \sin^2\theta_{13} = 0.02240; \quad \sin^2\theta_{23} = 0.582; \\ \delta_{\rm CP} = -2.50{\rm rad} \quad \Delta m^2_{21} = 7.39 \times 10^{-5}{\rm eV}^2 \quad \Delta m^2_{31} = 2.525 \times 10^{-3}{\rm eV}^2 \end{gathered} \tag{23}$$

  The baseline is 1300km for DUNE. We only need the value for the matter in the case of DUNE. I am using $\rho = 2.848 g/cm^3$.

- From reference [] we have **We divide the simulated data in energy bins of constant width $\Delta E_\nu = 0.5$ GeV, between 0 and 20 GeV, for our analyses**.

- Need to relate the plot with the reconstructed and true energy. Gaussian transformation?
  The differential rate

$$\frac{dN_{\rm events}^{\rm NSI}}{dE_\nu^{\rm true}} = \phi_\mu P_{\mu\tau}^{\rm NSI}\sigma_\tau = \frac{P_{\mu\tau}^{\rm NSI}}{P_{\mu\tau}^{\rm SM}}\frac{dN_{\rm events}^{\rm SM}}{dE_\nu^{\rm true}} \tag{24}$$

  in terms of true energy and the differential rate

$$\frac{dN_{\rm events}^{\rm NSI}}{dE_\nu^{\rm true}} = \phi_\mu P_{\mu\tau}^{\rm NSI}\sigma_\tau = \frac{P_{\mu\tau}^{\rm NSI}}{P_{\mu\tau}^{\rm SM}}\frac{dN_{\rm events}^{\rm SM}}{dE_\nu^{\rm true}} \tag{25}$$

  are connected by

$$\frac{dN_{\rm events}^{\rm NSI}}{dE_\nu^{\rm reco}} = \int \frac{dN_{\rm events}^{\rm NSI}}{dE_\nu^{\rm true}}\frac{{\rm d}\mathscr{R}}{{\rm d}E_\nu^{\rm reco}}(E_\nu^{\rm reco}, E_\nu^{\rm true})\,{\rm d}E_\nu^{\rm true} \tag{26}$$

  where

$$\frac{{\rm d}\mathscr{R}}{{\rm d}E_\nu^{\rm reco}}(E_\nu^{\rm reco}, E_\nu^{\rm true}) = \frac{1}{\sqrt{2\pi}\,\sigma_E}\exp\left[-\frac{1}{2}\left(\frac{E_\nu^{\rm reco} - bE_\nu^{\rm true}}{\sigma_E}\right)^2\right] \tag{27}$$

  with $\sigma_E = rE_\nu^{\rm true}, b = 0.45, r = 0.25$
  For an explanation of reconstructed and true energy[1]

[1] From GLOBES manual [9], section 10.1 we have the explanation of reconstructed and true energy.

Appendix A: EXTRA

in [1] they have (appendix A)

$$\sigma_E = 7\% \left(\frac{E_\nu}{1\mathrm{GeV}} \right) + 3.5\% \sqrt{\frac{E_\nu}{1\mathrm{GeV}}} \tag{A1}$$

For example in [10] they quote the following function

$$\frac{\mathrm{dR}}{\mathrm{d}N_h} = \frac{1}{\sqrt{2\pi}\,\sigma_h(T_e)} \exp\left[-\frac{1}{2} \left(\frac{N_h - \bar{N}_h(T_e)}{\sigma_h(T_e)} \right)^2 \right] \tag{A2}$$

As an example they use

$$\sigma_h(\bar{N}_h) = 1.21974 + 1.60121\sqrt{\bar{N}_h} - 0.14859\bar{N}_h. \tag{A3}$$

the transformation between reconstructed energy and true energy is given by

$$S^f_{N_h} = \int \frac{\mathrm{d}S^f_s}{\mathrm{d}T_e}(T_e)\, \frac{\mathrm{d}\mathscr{R}}{\mathrm{d}N_h}(T_e, N_h)\, \mathrm{d}T_e \tag{A4}$$

For us $\frac{\mathrm{d}S^f_s}{\mathrm{d}T_e}(T_e)$ is the spectrum as function of true energy, $S^f_{N_h}$ is spectrum in terms of reconstructed energy and $\frac{\mathrm{dR}}{\mathrm{d}N_h}$ is the resolution function.

in another words, we begin with spectrum of true energy and due the resolution we really observe the spectrum of the reconstructed energy. in reference [1] the Figure 2 of this paper have these two distributions. We reproduce here this figure in 1

- Assuming that the near detector is better than the far detector, we can use the same plot to study the tau neutrino flux in this case. We can just use the same plot, but now we set $L = 0$. This gives the number of events due to tau neutrino in our model (the expected number in the SM is zero.)

Appendix B: NOνA and T2K - Epsilon et and mut

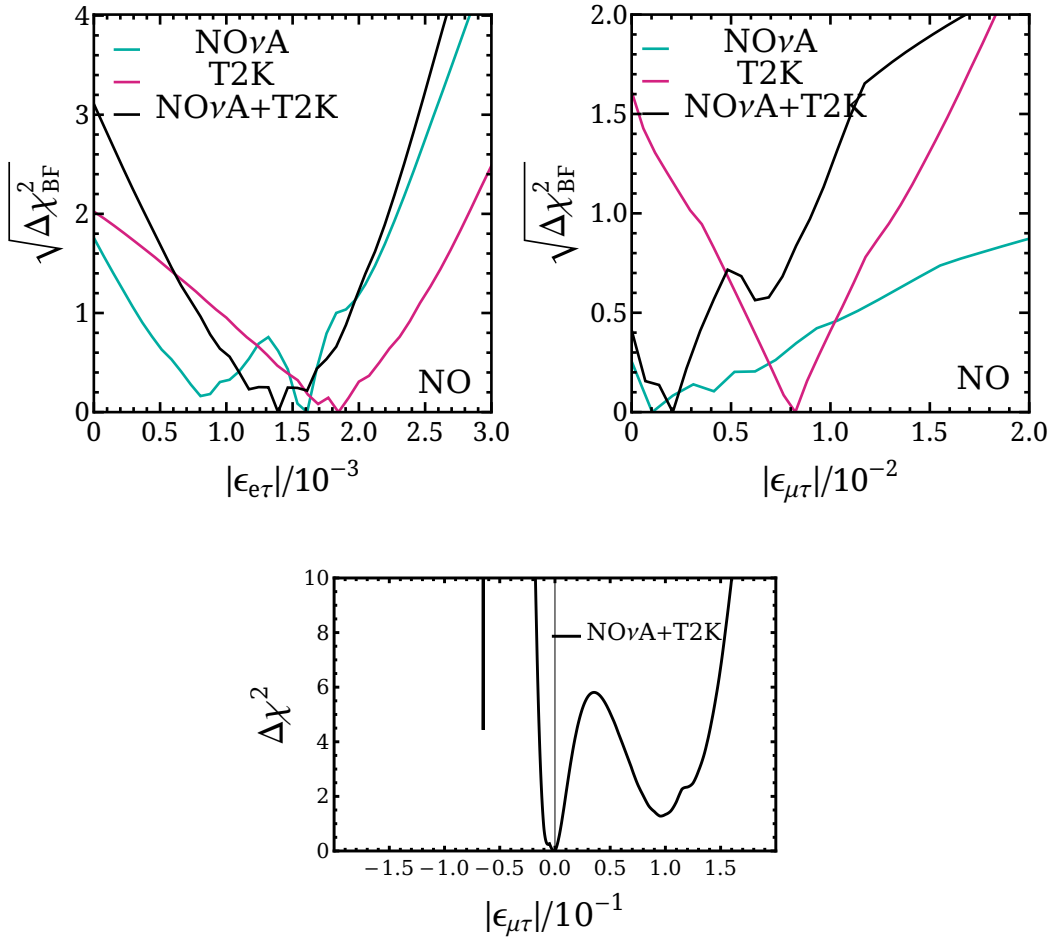

[1] A. De Gouvêa, K. J. Kelly, G. V. Stenico, and P. Pasquini, Phys. Rev. D **100**, 016004 (2019), arXiv:1904.07265 [hep-ph].
[2] A. Falkowski, M. González-Alonso, and Z. Tabrizi, JHEP **11**, 048 (2020), arXiv:1910.02971 [hep-ph].
[3] A. Falkowski, M. González-Alonso, J. Kopp, Y. Soreq, and Z. Tabrizi, JHEP **10**, 086 (2021), arXiv:2105.12136 [hep-ph].
[4] C. Giunti, C. W. Kim, J. A. Lee, and U. W. Lee, Phys. Rev. D **48**, 4310 (1993), arXiv:hep-ph/9305276.
[5] E. K. Akhmedov and J. Kopp, JHEP **04**, 008 (2010), [Erratum: JHEP 10, 052 (2013)], arXiv:1001.4815 [hep-ph].
[6] A. Kobach, A. V. Manohar, and J. McGreevy, Phys. Lett. B **783**, 59 (2018), arXiv:1711.07491 [hep-ph].
[7] L. Alvarez-Ruso *et al.* (NuSTEC), Prog. Part. Nucl. Phys. **100**, 1 (2018), arXiv:1706.03621 [hep-ph].
[8] V. Bresó-Pla, A. Falkowski, M. González-Alonso, and K. Monsálvez-Pozo, JHEP **05**, 074 (2023), arXiv:2301.07036 [hep-ph].
[9] P. Huber, J. Kopp, M. Lindner, M. Rolinec, and W. Winter, Computer Physics Communications **177**, 432–438 (2007).
[10] M. C. Gonzalez-Garcia, M. Maltoni, J. a. P. Pinheiro, and A. M. Serenelli, JHEP **02**, 064 (2024), arXiv:2311.16226 [hep-ph].